International Journal of Nanoelectronics and Materials

In Press, Accepted Manuscript – Note to user

Effect of Carbon Supports on Oxygen Reduction Reaction of Iron/Cobalt Electrocatalyst

S.A. Anuar[1], K.S. Loh[2,*], S. Samad[2], A.F. Zainul Abidin[2], W.Y. Wong[2], A.B. Mohamad[1,2], and T.K. Lee[1,3]

[1]Faculty of Engineering and Built Environment, Universiti Kebangsaan Malaysia, 43600 Bangi UKM, Selangor, Malaysia
[2]Fuel Cell Institute, Universiti Kebangsaan Malaysia, 43600 Bangi UKM, Selangor, Malaysia
[3]Department of Chemistry – Ångström Laboratory, Uppsala University, Box 538, SE-751 21 Uppsala, Sweden

ABSTRACT

Dual metal FeCo has great potential as Pt-free catalysts in various applications, such as cathodic catalysts for fuel cells, in order to reduce the cost significantly and make fuel cell commercialization viable. In this study, dual metal FeCo catalysts supported on carbon Vulcan XC-72, carbon nanotubes (CNT), and reduced graphene oxide (rGO) were successfully prepared via facile co-precipitation method with varying weight ratios of Fe and Co. The structure of the as-prepared catalysts was characterized by powder X-ray diffraction (XRD), scanning electron micrographs (SEM), and X-ray photoelectron spectroscopy (XPS). The XPS analysis revealed that $CoFe_2O_4$ were present on the catalyst particle surface with different Fe to Co ratio. The emergence of the new peak at 530.5 eV is assigned to the deposition of $CoFe_2O_4$, which is enabled via Fe-O-Co bonds. The FeCo/rGO catalyst with weight ratio of 2:1 exhibited the optimum performance for oxygen reduction reaction (ORR), with reduction peak of 0.163 mA cm^{-2} at 0.385 V vs. Ag/AgCl in an acidic media. The experimental result suggested that the dual metal FeCo catalyst display favorable electrocatalytic activity towards ORR and appears to be a promising cathodic electrocatalyst for an acidic fuel cell.

Keywords: Carbon supports, Electrocatalyst, Iron/cobalt, Oxygen reduction.

1. INTRODUCTION (First-level heading, Cambria 11pt, Uppercase, Bold)

Pt or Pt-based alloys are widely used as catalysts in fuel cells due to their effectiveness for cathodic oxygen reduction reaction (ORR) [1-4]. However, the use of Pt has its drawbacks where the cost of Pt is expensive, and susceptible to carbon poisoning in the presence of carbon monoxide [5-7]. During the past several decades, researchers have found that heat-treated Fe- and Co- based complexes are the most promising catalysts for the oxygen reduction reaction (ORR) in acidic media [8]. Numerous studies have been conducted in order to investigate bimetallic iron/cobalt (FeCo) with various modifications and functionalisations as ORR catalysts [9-12]. On the other hand, researchers have found that carbon supports, such as carbon black13, carbon nanotubes [14], activated carbon [15] or modified graphene [16], play an important role in improving both the ORR catalytic activity and the stability of metal and metal oxide species [17]. Recently, graphene has garnered significant interest due to its unique properties, such as excellent electrical conductivity, fascinating structure and high surface area [18]. Reduced graphene oxide (rGO) appears in sheets comprised of graphene domains interspersed with residual oxygen-containing functionalities, and the scalability of rGO synthesis has allowed for the production of numerous graphene-based materials with enhanced physical properties [19]. However, little study has been done on the effect of different Fe to Co ratios in FeCo catalysts supported on reduced graphene oxide.

*E-mail of corresponding author: ksloh@ukm.edu.my

In this study, dual metal FeCo catalysts with varying Fe to Co molar ratios (1:1, 1:2, 2:1) on different carbon supports, namely, activated carbon Vulcan XC-72 (denoted as C), carbon nanotube (CNT) or reduced graphene oxide (rGO), were synthesized chemical reduction method. The effect of different carbonaceous material as the support for FeCo have been investigated and correlated to their catalytic activity.

2. MATERIAL AND METHODS

2.1 Synthesis of FeCo/*x* (*x* = C, CNT, rGO)

Three difference carbon materials (C, CNT and rGO) were selected as FeCo catalyst support in this study. The Vulcan XC-72 and CNT (graphite powder 99% commercially obtained from Alfa Aesar) were used as received after several cycles of washing, rinsing and drying to remove any impurities. The rGO was prepared according to modified Hummer's method, as reported in our previous study [11].

To prepare FeCo/x (x = C, CNT, rGO) a:b (a:b = 1:2, 1:1, 2:1), different ratio of metal precursor, $Fe(SO)_4 \bullet 7H_2O$ and $Co(Cl_2)2 \bullet 6H_2O$, were dispersed into 4 mL of deionised water and stirred for 30 minutes at 30 °C using a hot plate to homogenize the solution. The mixture was the added to 20 mL (1 mg/mL) of an aqueous suspension of C, CNT or rGO. Then, 5 g of dissolved $NaBH_4$ solution was added, followed by vigorous stirring for another 30 minutes. The solution was then homogenized in a 60 °C water bath for 2 h, aided by ultrasonic dispersion. The final product was washed once with ethanol and 3 times with deionised water. The sample was dried at 80 °C for 24 hours in a vacuum oven. The total mass of FeCo prepared was kept at 0.15 g for comparison.

2.2 Characterization of FeCo Catalyst

The morphologies and microstructures of the FeCo catalysts were characterized by Field Emission Scanning Electron Microscopy (FESEM), using a Zeiss/SUPRA 55VP microscope, to observe the catalyst morphologies. X-ray Diffraction (XRD) was conducted using a Bruker/D8 Advance (λ = 1.54056 Å) on powder samples, with an Al-K_α sources, to analyse the crystallinity structures and compositions of the catalyst samples. X-ray Photoelectron Spectroscopy (XPS) analysis was carried out with a Kratos/Axis ultra DLD X-ray photoelectron spectrometer using Mg-K_α sources, to evaluate the chemical state and elemental composition of the catalyst surface.

2.3 Electrochemical Measurements

The working electrode which consist of FeCo catalyst was prepared for electrochemical measurement. The catalyst ink was formed by ultrasonically disperse of 5 mg of FeCo catalyst in 100 µL of Nafion® ionomer solution with 900 µL of deionised water. The catalyst was deposited onto the surface of a glassy carbon disk electrode (geometric area = 1.9635 cm^2). The catalyst loading was controlled at 396.8254 $mg_{catalyst}cm^{-2}$ unless stated otherwise. The ink coated electrode was dried for approximately 8 hours.

The FeCo samples coated on a glassy carbon (GC) electrode is used to conduct ORR measurements using cyclic voltammetry (CV) in acidic medium, using an Autolab PGSTAT128N Potentiostat/Galvanostat. The electrochemical analysis was carried out in a three-electrode system set-up, where the Ag/AgCl served as the reference electrode; Pt wire as the counter electrode; and glassy carbon as the working electrode. Unless stated otherwise, all potentials reported here in this paper are referred to the Ag/AgCl (saturated KCl) reference electrode. The

ORR activity of the catalysts was characterized by cyclic voltammetry, with a potential range from 0 to 1.0 V at a scan rate of 10 mVs^{-1}. All the electrochemical measurements were carried out with 0.5 M H_2SO_4 O_2-purged electrolyte solution at room temperature. Prior to this, a background measurement was conducted with N_2-saturated electrolyte. The overall methodology approach is representing in Figure 1.

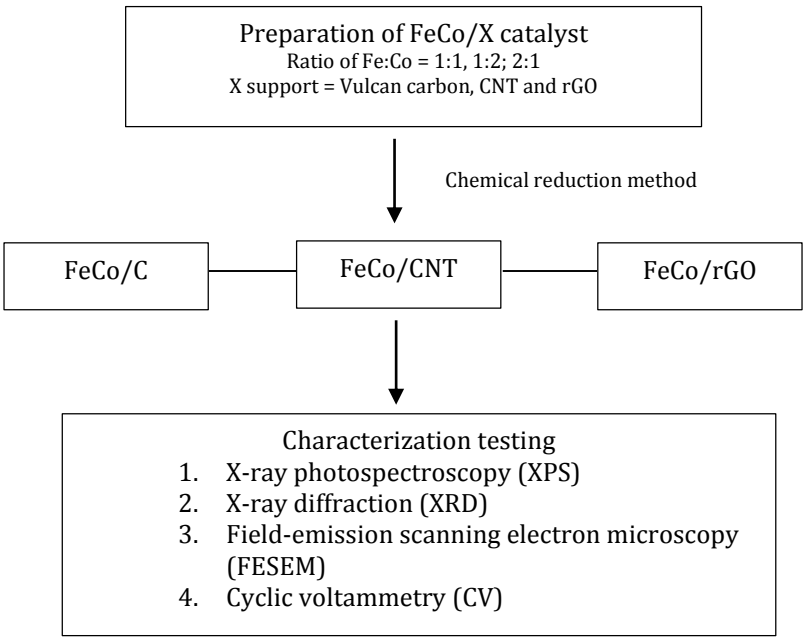

Figure 1. Schematic diagram of methodology.

3. RESULTS AND DISCUSSION

3.1 XPS Analysis

The chemical compositions and structures of the FeCo catalysts were investigated by XPS. As shown in Figure 2, the wide scan revealed the presence of C1s, O1s, Fe2p and Co2p at binding energies of ~285.6, 532.5, 712.9 and 782.4 eV, respectively, which is similar to the binding energies report by Jin et al. [20]. The presence of Fe 2p and Co 2p peaks indicates the successful incorporated of Fe and Co into all of the carbon supports [21]. As report by Samad et al. [11], the binding energies of 781.8 and 796.4 eV can be attributed to Co $2p_{3/2}$ and Co $2p_{1/2}$.; whilst the binding energies of 711.5 and 724.4 eV can be attributed to Fe $2p_{3/2}$ and Fe $2p_{1/2}$, respectively. Table 1 shows the catalyst composition (% weight) calculated from the XPS spectra.

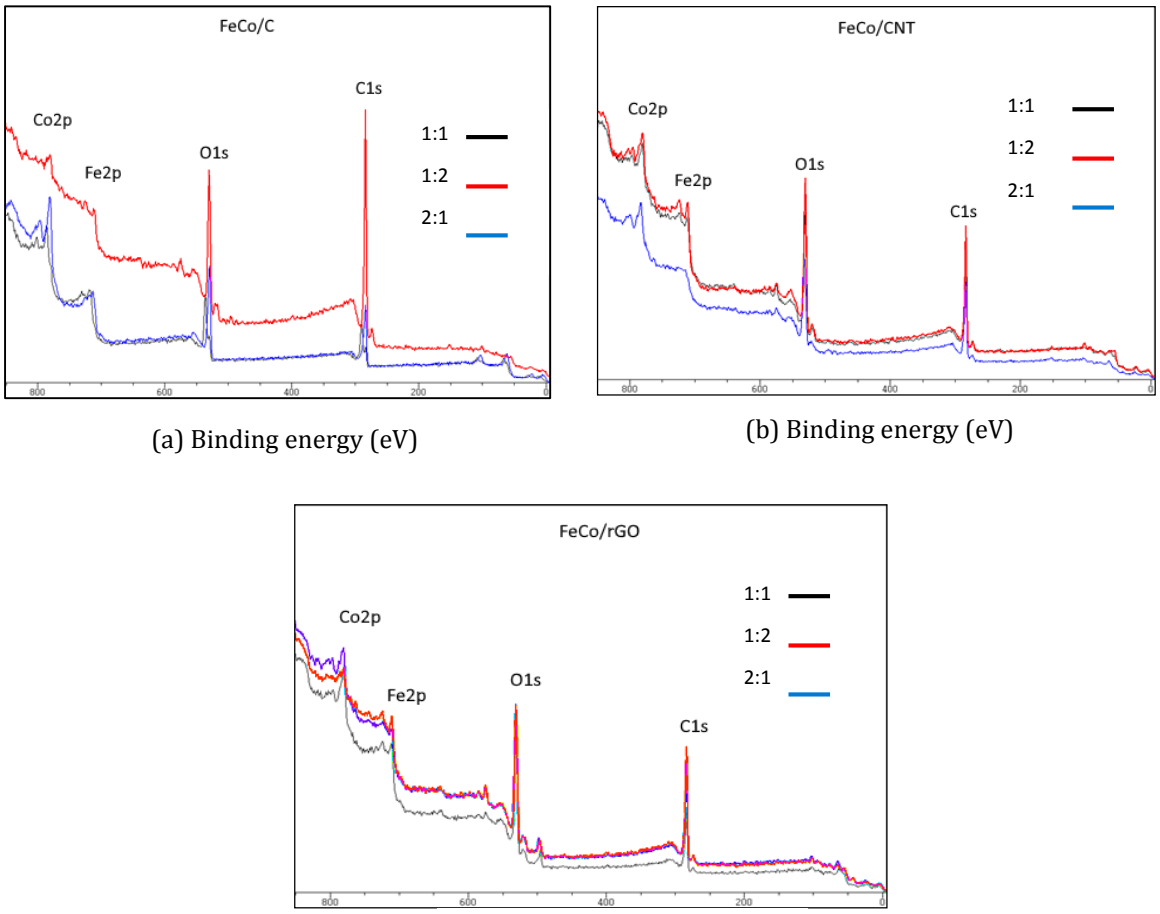

(a) Binding energy (eV)

(b) Binding energy (eV)

(c) Binding energy (eV)

Figure 2. XPS Wide scan of (a) FeCo/C, (b) FeCo/CNT and (c) FeCo/rGO catalyst samples.

Table 1 Elemental composition for selected catalysts (% weight) obtained from XPS spectra

Catalyst	% weight				Fe/Co ratio
	C	O	Fe	Co	
FeCo/C 1:2	22.82	17.11	20.47	39.60	0.52
FeCo/C 1:1	25.63	20.43	26.19	27.75	0.94
FeCo/C 2:1	40.83	19.79	20.18	19.21	1.05
FeCo/CNT 1:2	15.51	17.58	41.05	25.86	1.59
FeCo/CNT 1:1	26.27	22.64	22.17	28.92	0.77
FeCo/CNT 2:1	21.21	21.67	26.40	30.73	0.86
FeCo/rGO 1:2	24.60	25.71	20.61	29.08	0.71
FeCo/rGO 1:1	20.85	22.87	29.03	27.25	1.07
FeCo/rGO 2:1	23.48	21.50	26.29	28.72	0.92

3.2 XRD

Figure 3 shows the XRD patterns for GO substrate, FeCo/CNT 2:1, FeCo/C 2:1 and FeCo/rGO 2:1 catalyst. The FeCo catalysts with ratio 2:1 are selected for further analysis as it already shown a better intensity compared with other samples. The major peaks for the catalyst sample

corresponded to a cubic spinel phase of cobalt ferrite, $CoFe_2O_4$, with a crystallographic facet of (220), (311), (400), (422), (511) and (440) (PDF Card No: 01-074-6403), were observed at 2θ = 30.1°, 35.4°, 43.5°, 53.6°, 56.9° and 62.5°, respectively. The peak intensity also varies according to the carbon supports, in the order of FeCo/C 2:1 > FeCo/CNT 2:1 > FeCo/rGO 2: 1. The calculated crystallite sized using Scherrer's equation is found to be as 25 nm.

In contrast with other carbon materials, only one sharp peak at 34.96° is presented in the FeCo/rGO 2:1 with using rGO as support, suggesting that the structure of this catalyst is almost amorphous, or of low crystallinity [17]. Furthermore, the absence of peaks at 10.66° and 26.4°, which are attributed to the (001) reflection of GO and (002) reflection of graphite, also confirmsed the reduction of GO to rGO [17,19]. The broadening of some peaks may be due to the macroscopic residual stress caused lattice distortion [12].

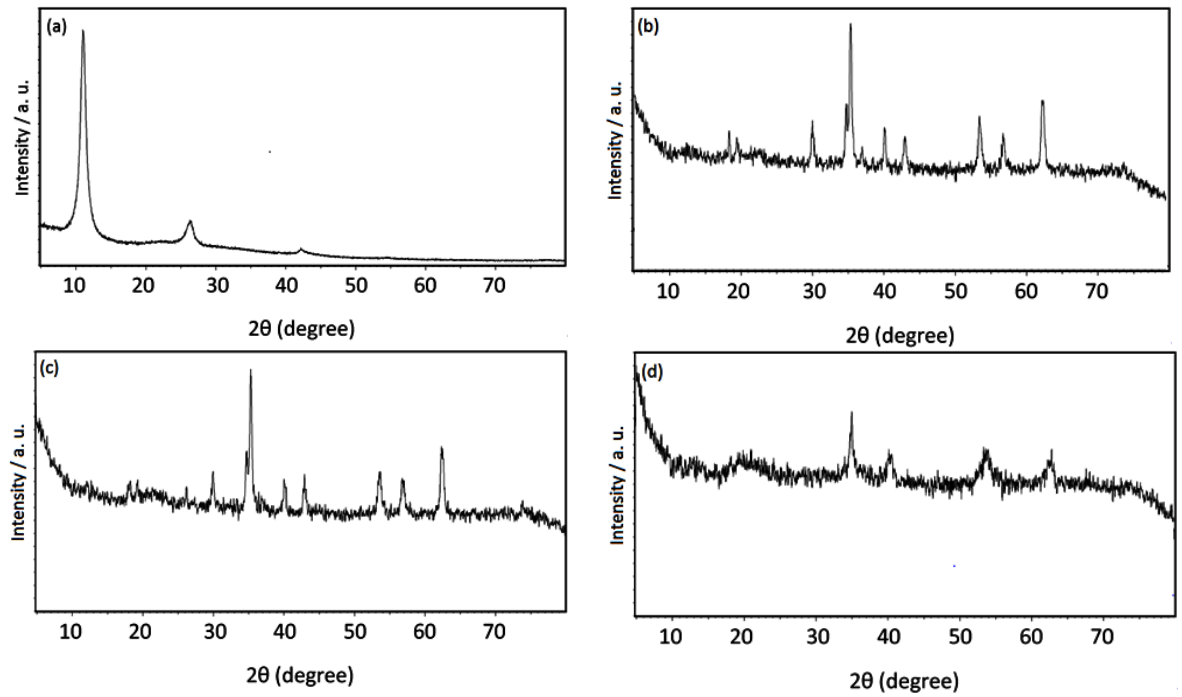

Figure 3. XRD spectrum of (a) GO, (b) FeCo/C 2:1, (c) FeCo/CNT and (d) FeCo/rGO 2:1

3.3 FESEM

Due to dipolar interactions between the magnetite nanoparticles, all FESEM images (Figure 4) at 200 nm magnification show aggregates of smaller, spherical-like CoFe2O4 particles. Figure 4 shows the morphologies of FeCo/C, FeCo/CNT and FeCo/rGO, with a Fe:Co metal composition of 2:1. Carbon Vulcan XC-72 has a very distinct morphological feature, with average diameter of 100 nm (Figure 4(a)). Due to acid washing during the preparation of FeCo/CNT 2:1, the CNTs exhibit a rough texture, as seen in Figure 4(b). The distribution of external diameters for the CNTs ranges from 150 to 200 nm. The tips of these CNTs are closed [22] and contain the catalytic particles (FeCo, $CoFe_2O_4$) on their surface. Figure 4(c) shows the SEM images for FeCo/rGO 2:1. Most of the FeCo nanoparticles are evenly distributed on the surface of the rGO nanosheets, as observed by Fan and co-workers in 2015 [23]. Due to the electrostatic interaction between Fe^{2+}, Co^{2+} and GO (COOH-, OH-), it was proposed that Fe^{2+} and Co^{2+} were attracted to the GO surface and facilitated the simultaneous reduction of FeCo nanoparticles and GO in situ, which served as the initial nucleation sites and optimal load position [24]. It has been shown that graphene sheets are distributed between the nanoporous composite with a large amount of void space, as stated by Yao and co-workers [25]. The dispersion of FeCo nanoparticles on the surface of rGO nanosheets

as nanoscale spacers also prevents the agglomeration of rGO nanosheets [21]. Figure 4(c) provides an example in which FeCo nanoparticles are dispersed, covered and wrapped by the flexible rGO nanosheets [12,25].

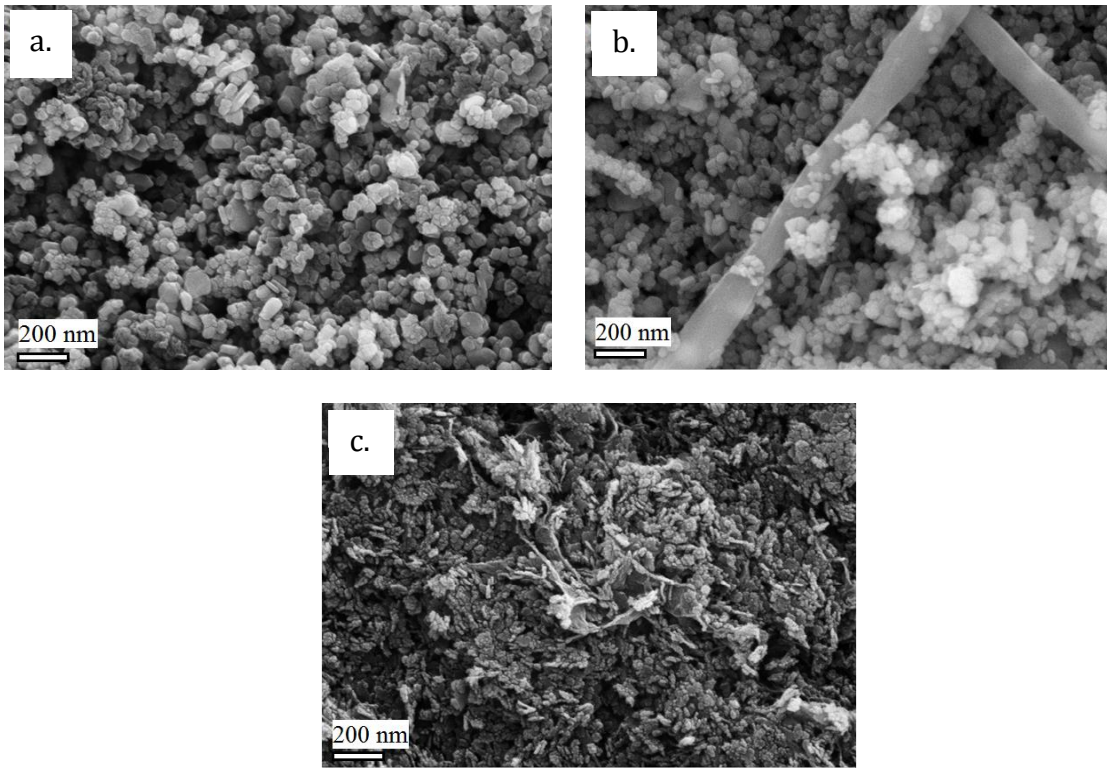

Figure 4. FESEM images of (a) FeCo/C 2:1, (b) FeCo/CNT 2:1, (c) FeCo/rGO 2:1 at 200 nm

3.4 ORR Activity of the FeCo Catalysts

To evaluate the electrocatalytic activity towards the ORR by the FeCo catalysts, CV measurements were conducted (Figure 5). All potentials were recorded vs. Ag/AgCl (saturated KCl) reference electrode. A well-defined oxidation and reduction peaks with varying current densities was observed in each of the catalyst voltammogram. This indicates a distinct sensitivity towards the ORR process by the catalysts, but with varying catalytic activities [17]. The anodic and cathodic peak current arises may cause from the redox reactions of Fe^{3+}/Fe^{2+}, and/or surface oxide formation due to the hydroquinone-quinone redox couple on the support surface [26]. This indicates that oxidized groups, including carboxyl, hydroxyl and carbonyl, were generated on the surface of carbon [27].

In Figure 5, the current densities measured for FeCo/C and FeCo/rGO were 0.1202 mA cm^{-2} and 0.1630 mA cm^{-2}, respectively. The higher current density observed for FeCo/rGO is likely due to the amourphous nature (with a better conduction path) that allows for easier electron transport (as observed in SEM and XRD). For the CNT and C supported FeCo, a higher onset and peak potential was observed, which is attributed to a better ORR catalytic reaction. This is likely due to the presence of the crystallite phase in CNT and C, which is not found in rGO, based on the XRD spectrum. However, the difference in the reduction peak for FeCo/CNT is insignificant because CNT is difficult to oxidize [24]. This indicates that changes in the Fe to Co metal ratio will not significantly alter the ORR performance by CNT, but for carbon Vulcan XC-72 and rGO, the catalytic performance increases proportionally with an increase in Fe. Thus, Fe to Co ratio of 2:1 was selected as the optimal ratio for the fabrication of FeCo catalysts on all carbon Vulcan XC-72,

CNT and rGO supports. Meanwhile, FeCo/rGO 2:1 exhibited the greatest electrochemical activity toward oxygen reduction in acidic medium, with the highest peak current density of 0.1630 mA cm^{-2}. This indicates that more oxygen molecules are absorbed and reduced on the surface of the catalyst [12]. In this hybrid, it is believed that the rGO sheets not only serve as a conduction path for shuttling electrons but also act as an active site for the ORR [28]. Varying the metal ratio alters the position of the peak potential on each support. In contrast to the work of Li and co-workers [10], the change in the potential position found in this study indicates that the interaction between the Fe and Co ions is significant.

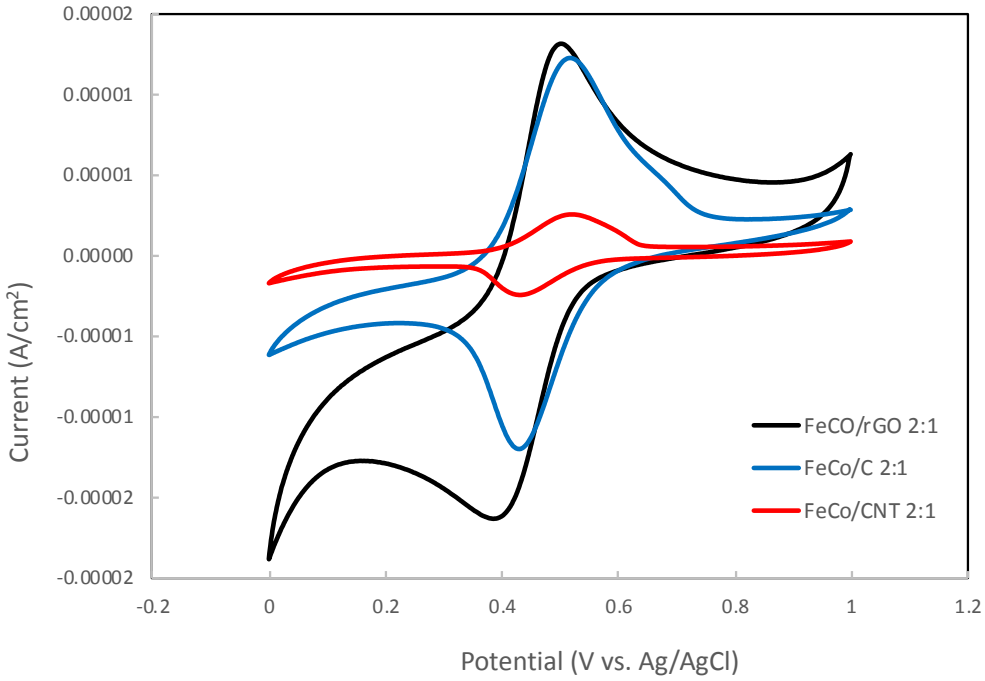

Figure 5. Cyclic voltammogram of FeCo/C, FeCo/CNT and FeCo/rGO samples in an O_2-saturated 0.5 M H_2SO_4 solution

4. CONCLUSION

In summary, FeCo catalysts were successfully prepared by a co-precipitation method and were characterized by XRD, XPS and SEM. The catalytic activity of the FeCo catalysts with various carbon supports toward the ORR in acidic medium was explored, and the efficient electrochemical catalytic reduction of oxygen was observed. Further experiments indicated that the ORR catalytic activity of the FeCo/x catalysts is sensitive to the ratio of Fe to Co present during synthesis. Based on these results, FeCo/rGO with a Fe:Co metal composition of 2:1 was shown to have the highest catalytic activity for the ORR in acidic medium and therefore has the potential to replace the current commercially available, high cost Pt-based catalysts for fuel cell applications.

ACKNOWLEDGEMENTS

This work is supported by the Universiti Kebangsaan Malaysia through the Universiti Research Grant (DIP-2017-024).

REFERENCES

[1] Peera, S. G., Lee, T. G., Sahu, A. H. Sustain. Energy Fuels. vol **3**, issue 8 (2019) pp. 1866-1891.
[2] Wu, D., Shen, X., Pan, Y., Yao, L., Peng, Z. ChemNanoMat. (2019) pp.201900319.
[3] Yi, S., Jiang, H., Bao, X., Zou, S., Liao, J., Zhang, Z. J. Electroanal. Chem. vol **848** (2019) pp.113279.
[4] Samad, S., Loh, K. S., Wong, W. Y., Lee, T. K., Surnarso, J., Chong, S. T., Daud, W. R. W. Int. J. Hydrogen Energy. vol **43,** issue 16 (2018) pp.7823-7854.
[5] Liang, Y., Dai, H., Zhou, J., Regier, T., Li, Y., Wang, H., Wang, J. Nature Mater. vol. **10**, (2011) pp. 780-786.
[6] Deak, D. V., Singh, D., King, J. C., Ozkan, U. S. Appl. Catal. B. vol **113-114,** (2012) pp. 126-133.
[7] Zhang, G., Lou, X. W., Wang, X., Xia, B. Y. Adv. Mater. vol **26,** issue 15 (2014) pp. 2408-2412.
[8] Liu, Q., Cao, S., Qiu, Y. Int. J. Hydrogen Energ. vol **42**, issue 49 (2017) pp. 29274-29282.
[9] Li, G., Zheng, K., Xu, C. Appl. Surf. Sc. vol. **487,** (2019) pp. 496-502.
[10] Li., S., Zhang, L., Kim, J., Pan, M., Shi, Z., Zhang, J. Electrochim. Acta. vol **55,** (2010) pp.7346-7353.
[11] Samad, S., Loh, K. S., Wong, W. Y., Sudarsono, W., Lee, T. K., Daud. J Alloys. Compd. vol **816,** (2020) pp.152573.
[12] Zhang. J., Wang, X., Qin, D., Xue, Z., Lu, X. Appl. Surf. Sc. vol **320,** (2014) pp. 73-82.
[13] Faubert, G., Lalande, G., Cote, R., Guay, D., Dodelet, J. P., Weng, L. T., Bertrand, P., Denes, G. Electrochim. Acta. vol **41,** issue 10 (1996) pp.1689-1701.
[14] Lu, M., Kharkwal, S., Ng, H. Y., & Li, S. F. Y. Biosens. Bioelectron. vol **26,** issue 12 (2011) pp. 4728-7732.
[15] Ma, Y., Wang, H., Ji, S., Goh, J., Feng, H., Wang, R. Electrochim. Acta. vol **133,** (2014) pp.391-398.
[16] Liang, Y., Li, Y., Wang, H., Zhou, J., Wang, J., Regier, T., & Dai, H. Nature Mater. vol **10,** issue 10 (2011) pp. 780-786.
[17] Lu, L., Hao, Q., Lei, W., Xia, X., Liu, P., Sun, D., Wang, X. Yang, X. (2015). Small. vol **11,** issue 43 (2015) pp.5833-5843.
[18] Nonoselov, K. S., Geim, A. K., Morozov, S. V., Jiang, D., Zhang, Y., Dubunos, S. V., Grigorieva, I. V., & Firsov, A. A. Science. vol **306,** (2004) pp. 666-669.
[19] Compton, O. C., Nguyen, S. T. Small. **vol 6,** issue 6 (2010) pp.711-723.
[20] Jin, X., Jiang, Y., Hu, Q., Zhang, S., Jiang, Q., Chen, L., Xu, L., Xie, Y, Huang, J. RSC Adv. vol **7,** (2017) pp.5637
[21] Bai, S., Shen, X. P., Zhu, G. X., Li, M. Z., Xi, H. T., & Chen, K. M. ACS Appl. Mater. Interfaces. vol **4,** issue 5 (2012) pp.2378-2386.
[22] Chen, J., Li, Y., Huang, L., Li, C., & Shi, G. Carbon. vol **81,** (2014) pp. 826-834.
[23] Fan, X., Gao, H., Kou, X., Zhang, B., & Wang, S. Mater. Res. Bull. vol **65,** (2015) pp.320-324.
[24] Hoyos-Palacio, L. M., Garcia, A. G., Perez-Robles, J. F., Gonzalez, J., Martinez-Tejada, H.V. Mater. Sc. and Eng. vol **59,** (2013) pp. 012005.
[25] Yao, B., Ding, Z., Feng, X., Yin, L., Shen, Q., Shi, Y., & Zhang, J. Electrochim. Acta. vol **148,** (2014) pp.283-290.
[26] Wang, Z., Lim, K., Zhang, H. S., Goh, V. L., Ng, J. L., Kuok, S. C. M. H., & Tang, S. L. Nano Lett. vol **6,** (2006) pp.1083-1086.
[27] Hou, Y., Huang, T., Wen, Z., Mao, S., Cui, S., Chen, J. Adv. Energ. Mater. vol **4,** (2014) pp.1400337.
[28] Hou, Y., Wen, Z., Cui, S., Ci, S., Mao, S., & Chen, J. Adv. Funct. Mater. vol **25,** issue 6, (2014) pp.872-882.